Vol. 501: 25–40, 2014
doi: 10.3354/meps10688

MARINE ECOLOGY PROGRESS SERIES
Mar Ecol Prog Ser

Published March 31

Marginal impacts of rising temperature on Arctic benthic microalgae production based on *in situ* measurements and modelled estimates

Jana Woelfel[1,2,*], Anja Eggert[3], Ulf Karsten[2]

[1]Leibniz Institute for Baltic Sea Research, Department of Marine Chemistry, Trace Gases, 18119 Rostock, Germany
[2]University of Rostock, Institute of Biological Sciences, Applied Ecology and Phycology, 18059 Rostock, Germany
[3]Leibniz Institute for Baltic Sea Research, Department of Physical Oceanography and Instrumentation, Theoretical Oceanography and Numerical Modelling, 18119 Rostock, Germany

ABSTRACT: Arctic microphytobenthic *in situ* net community production (NCP) was measured via the oxygen exchange rate in benthic chambers equipped with optical sensor spots at 3 representative sandy sites in Kongsfjorden (Svalbard, 79° N, 12° E) at 3 to 11 m water depth during June 2008. No significant differences were detected between stations and depths in either photoautotrophic biomass or primary production. All sites showed low but variable rates of NCP, ranging from −0.3 to +0.6 mmol O_2 m^{-2} h^{-1} (−9 to +18 mg O_2 m^{-2} h^{-1}). The numerical model of Walsby (1997) was applied to estimate seasonal and regional rates of nearshore NCP for 2008 using *in situ* *P/E* curve parameters, solar global radiation, wind data and satellite-derived sea surface temperatures. The highest daily NCP rates of 15 to 18 mmol O_2 m^{-2} d^{-1} were found throughout the Arctic spring and summer seasons (1 April until 31 August 2008) at shallow depths <15 m. The differences between modelled stratified and fully mixed water column conditions were small and in the range of 10%. Depth- and time-integrated NCP of the entire Kongsfjorden coastline during June 2008 yielded 9 t of O_2. A predicted increase in the sea surface temperature by 2°C would have only a marginal impact on the NCP (<3%). Our model sensitivity analysis of the uncertainties associated with *P/E* curve parameters and Q_{10} values clearly showed a crucial dependence of NCP on the Q_{10} values. Thus, further studies on temperature dependence are required.

KEY WORDS: Arctic benthic diatoms · Respiration and net production · Biomass · Sediment characteristics · Benthic chambers · Kongsfjorden

INTRODUCTION

The important worldwide ecological roles of microphytobenthos as sediment stabilisers and a biomass resource for grazers has been recognised (e.g. reviewed in MacIntyre et al. 1996, Cahoon 1999). Microphytobenthic primary production from cold to warm waters has been thoroughly investigated; an increasing number of studies have shown that benthic microalgae contribute significantly, up to 50%, to primary production in subtidal sediment ecosystems (e.g. Tagus Estuary, Portugal in Brotas et al. 1995; different estuaries and tidal flats reviewed in Underwood & Kromkamp 1999). Similar studies in polar regions remain scarce (Glud et al. 2009, Woelfel et al. 2010), mainly due to the logistical constraints of high-latitude work. Glud et al. (2009) evaluated 10 peer-reviewed and 3 unpublished studies on polar benthic microalgal production and showed that benthic production typically exceeded pelagic productivity by a factor of 1.5 in 30 m or less. Consequently, phytobenthos and particular microphytobenthos are thought to have an exceptionally important role in polar coastal food webs. In this region, they may pro-

*Corresponding author: jana.woelfel@io-warnemuende.de

vide an exclusive food source for benthic grazers, as only a minor fraction of phytoplankton biomass reaches the sediments (Rysgaard et al. 1999).

Global climate change impacts the whole Arctic ecosystem. The Arctic is projected to warm, on average, by 5°C over the next century, which is more than most other global areas (Intergovernmental Panel on Climate Change scenario A1B in Christensen et al. 2007). However, winter temperatures will increase by >7°C, while summer temperatures may only increase by 2 to 4°C (MacDonald 2010). Arctic warming is accompanied by a negative balance between the Arctic glaciers and reductions in the area and thickness of ice (sea and river) and snow cover. For example, the September 2010 (annual minimum) sea-ice extent in the Arctic basin was the third smallest ever recorded (Forbes 2011). In 2007, the ice-cover minimum reached a record low of 4.28 million km^2, 39% below the long-term mean (1979–2000, Stroeve et al. 2007). Ice-cover decrease is accompanied by rising light availability in the water column and is expected to stimulate benthic primary production. Annual pelagic production of the Arctic Ocean has already increased annually by 5 to 6% as a consequence of enhanced light availability (Arrigo et al. 2008). Sakshaug (2004) estimated that Arctic pelagic annual primary production will increase by a factor of 3.5 (from <40 g C m^{-2} yr^{-1} to 100–150 g C m^{-2} yr^{-1}) if the sea ice disappears in the Arctic part of the Barents Sea and on the Bering Shelf. We also expect benthic primary production to increase in intensity, space and time in the Arctic region. Thus far, the effects of changes in both temperature and underwater light on Arctic marine benthic primary production have scarcely been investigated; therefore, more field work and modelling approaches are urgently needed to make realistic predictions.

Our previous study indicated that Arctic microphytobenthic potential gross production (sum of dark community consumption and net production, measured *ex situ* in sediment cores of the Kongsfjorden, Svalbard) is similar to production in temperate regions (Woelfel et al. 2009a). However, a transfer and interpretation of *ex situ* data to changing natural light conditions was lacking from that study. We then developed chambers with optical oxygen sensors to measure *in situ* benthic oxygen exchange rates and applied this set-up for the first time in a polar habitat. We were able to measure *in situ* area-integrated net community production (NCP) of microphytobenthos at 3 representative sites with different water depths in Kongsfjorden (Svalbard) in June 2008. We constructed a regional photosynthesis versus irradiance (P/E) curve from the *in situ* measurements. Based on its parameterisation, we modelled regional NCP of the entire Kongsfjorden for the Arctic spring and summer (1 April until 31 August 2008). Additionally, we analysed the quantitative effect of the proposed increase in sea surface temperature of 2°C on microphytobenthic primary production according to predictions for summer warming until 2100 in Kongsfjorden (MacDonald 2010).

MATERIALS AND METHODS

Study sites and environmental conditions

The field study was performed in June 2008 in Kongsfjorden (79° N, 12° E) on the west coast of Svalbard (Fig. 1). Kongsfjorden is a deep fjord with a maximum depth of 400 m. It extends 26 km from the northwest to the southeast and is 3 to 8 km wide. The fjord is influenced by the presence of 4 tidewater glaciers (Fig. 1). The tidal range is ~2 m (Svendsen et al. 2002). The annual mean water temperature is ~0°C, but sea surface temperatures during the Arctic summer can reach 4 to 6°C due to the influence of the warm water masses of the Westspitsbergen Current (Hanelt et al. 2001). The inner part of Kongsfjorden usually becomes ice-covered by December or January, but complete ice cover is an exceptional event. The fjord is typically completely ice-free by the end of May (Svendsen et al. 2002).

Three stations along the shoreline were investigated: Nansenbay (NAT), Brandal (BRL) and London (LON). Stns NAT and BRL were located 200 and 1000 m from Ny Ålesund harbour, respectively, at an exposed site of the southern shore. Stn LON was located at the northern shore and was more sheltered due to its location in a small inlet (Fig. 1). These stations are representative of Kongfjorden's sandy coastal areas, but they were chosen primarily for their ease of accessibility and for comparison with previous studies (Woelfel et al. 2009a, 2010). A more detailed description of the stations is given in Woelfel et al. (2009a).

At LON and BRL, *in situ* measuring and sampling were performed simultaneously at 3 and 7 m water depth. Three water depths (4, 6 and 11 m) were investigated at NAT. The temperature and salinity of the surface water (≤1 m) were measured 3 to 7 times a day, always when primary productivity was measured. Salinity was measured as conductivity using the practical salinity scale using a WTW Salinometer Multiline P4 (WTW GmbH). Sediment grain size had

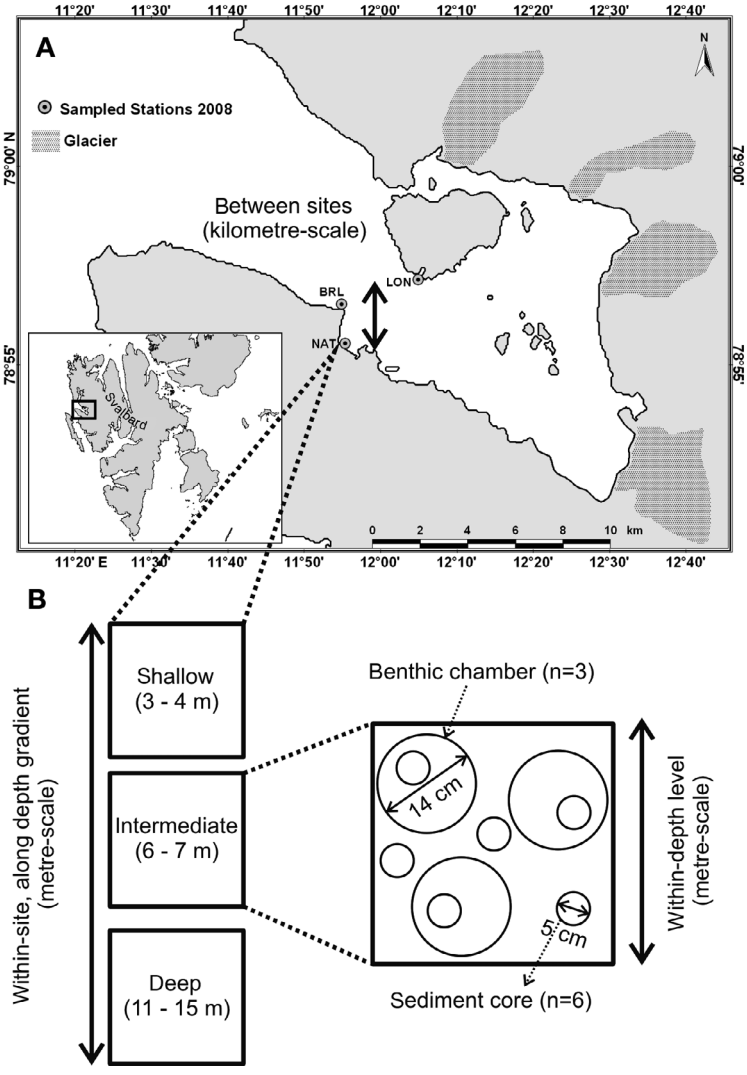

Fig. 1. (A) Location of the 3 sampling stations Nansenbay (NAT), London (LON) and Brandal (BRL) in Kongsfjorden. The location of Kongsfjorden in Svalbard is shown on the inset map. The 4 adjacent glaciers are shown as dark grey areas. (B) Schematic representation of the sampling design, i.e. the depth gradient sampled at each station and the sampling units within each station and depth level

been determined earlier in 2006 (Woelfel et al. 2009a), and as a control, water content was measured as weight lost after drying the weighed sediment samples for 24 h at 105°C.

Underwater planar light and temperature loggers (HOBO® Pendant, Onset Computer Corporation; accuracy: ±0.53°C from 0° to 50°C) were positioned at each water depth. The instantaneous value for underwater irradiance and temperature was logged every 10 to 20 s during each measuring event. The HOBO sensor (unit = lux, 150 to 1200 nm) was calibrated once against a quantum sensor (unit = µmol photons m^{-2} s^{-1} photosynthetically active radiation [PAR], 400 to 700 nm) (R. Marquardt unpubl. data). Continuous measurements of surface and subsurface irradiance were performed by means of a HOBO Pendant logger and a LiCor 1000 (LiCor) data logger equipped with a spherical (underwater) and a cosine-corrected (surface) PAR-sensor (LiCor).

As an indicator of the optical properties of the seawater, the diffuse vertical attenuation coefficient of downwelling irradiance (K_d, m^{-1}) was determined at the 3 sites (BRL, LON, NAT) by measuring the underwater downwelling irradiance at 2 water depths logged every 10 min (BRL and LON: z_1 = 3 m and z_2 = 7 m water depth; NAT: z_1 = 3 m and z_2 = 11 m water depth).

Measurements of dark community consumption and net community production

In situ benthic oxygen exchange rates were measured in 6 chambers with 2 different dimensions (Fig. 2; large chamber height: 300 mm; small chamber height: 200 mm; diameter of both: 140 mm). Chambers were deployed at 50 mm sediment depth; the large

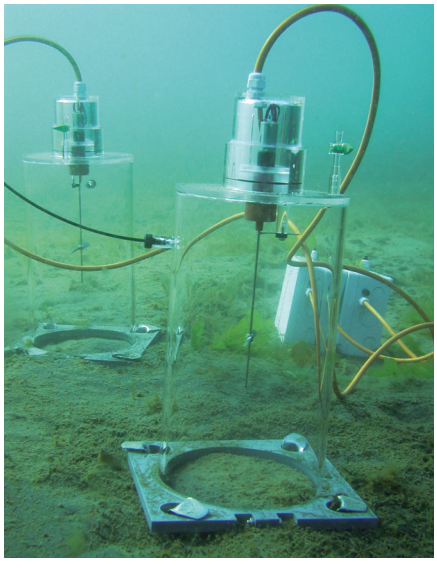

Fig. 2. Underwater benthic air tight Plexiglas® chamber (maximal 300 mm height, inner diameter 140 mm). At the top is a motor for the stirring device with the battery and the filling port. On the left is the planar oxygen sensor spot with an optical fibre. Photographer: Michael Bartz

chambers had a volume of 3.9 l, and the small chambers had a volume of 2.3 l. Each chamber was equipped with a 30 mm internal stirring propeller (driven by an external rotating motor at 20 to 30 rpm), which guaranteed optimal mixing of the water inside. Oxygen concentrations were determined in the sediment near the water layer with commercial PSt3 planar oxygen sensor spots (located within the chamber >10 cm above sediment; diameter 5 mm; accuracy ± 0.4 % O_2 at 20.9 % O_2) in combination with a Fibox 3 measuring device (PreSens GmbH). A planar oxygen sensor spot was glued to the inner wall of each benthic chamber, and the decrease or increase of the luminescence signal was recorded online. Calibrations were performed in aerated ambient seawater (100 % atmospheric saturation) and in saturated sodium dithionite solution in seawater (0 % oxygen).

At each site and water depth, SCUBA divers manually pushed 3 benthic chamber replicates ~50 mm into the sediment (Fig. 2). The 2 water depths at LON and BRL were investigated simultaneously by mounting the large chambers at 3 m and the small chambers at 7 m water depth. At Stn NAT, 3 water depths were studied: 3 and 11 m were measured simultaneously, and 6 m was investigated subsequently.

At the beginning of each measuring event, chambers were fixed at the bottom, the stirrers were started and the optical microfiber from each chamber was connected to a buoy at the water surface. Dark community composition (DCC) was measured in chambers that were darkened with thick black bin liners during the first 24 h. The chambers were then exposed to ambient light for up to 48 h to measure NCP (whole incubation period: 72 to 80 h). The prevailing oxygen data were recorded at intervals of 2 to 8 h depending on weather conditions. Rates of DCC and NCP were calculated from the slopes of oxygen evolution averaged over the whole incubation period: for DCC within 24 h darkness and for NCP within 48 to 56 h light (the duration of light exposure was different between measurement events due to logistical reasons). Gross community production (GCP) rates were calculated as the sum of the DCC and NCP rates. All oxygen exchange rates were transformed into carbon equivalents assuming a photosynthetic quotient (PQ = $\Delta O_2/\Delta C$) of 1 (Hargrave et al. 1983).

A regional *P/E* curve of NCP vs. photon flux density (PFD) was constructed from all measured *in situ* O_2 exchange rates (Fig. 3). The respective mean irradiances of each measurement interval (2 to 8 h) were used to parameterise the *P/E* curve using Eq. (1) (Webb et al. 1974):

$$NCP(PFD) = NCP_{max}\left(1 - e^{\frac{-\alpha \cdot PFD}{NCP_{max}}}\right) + DCC \quad (1)$$

The light saturation point E_k used as an index of light acclimation was calculated as NCP_{max}/α. The least square estimators of the maximum rate of net community production (NCP_{max}), the light utilisation coefficient (α) and the rate of DCC were estimated with the Levenberg-Marquardt iteration algorithm.

After removing the benthic chambers, the sediment underneath was sampled for further analysis of phototrophic biomass (chlorophyll *a* concentration) and organic content (particulate organic carbon and nitrogen).

Due to high patchiness of benthic biomass within the area of the chambers (diameter = 140 mm), 6 replicates were taken from each site (1 from each

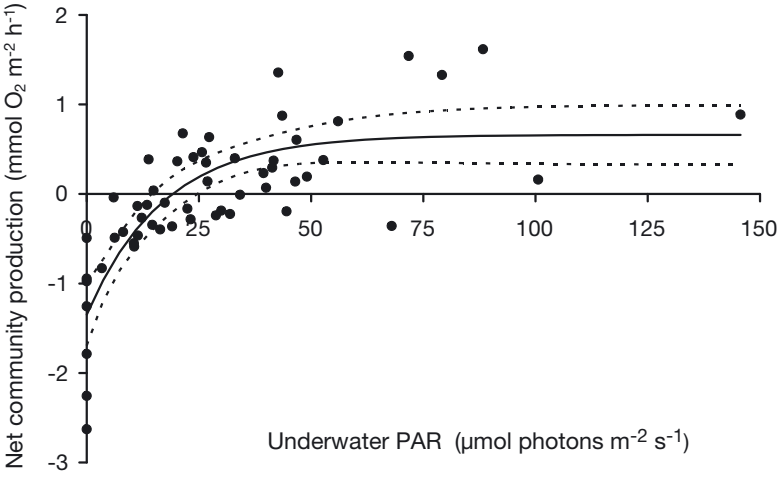

Fig. 3. *P/E* curve of all 55 net community production (NCP) rates measured as *in situ* O_2 exchange rates (mmol O_2 m^{-2} h^{-1}) at *in situ* photon flux densities (PFDs) of photosynthetically active radiation (PAR; µmol photons m^{-2} s^{-1}). All O_2 exchange rates (n = 3; LON_3 n = 1) of the 3 sampling stations and irradiance data (sampling rate 15 to 20 s) were calculated as mean of each measurement interval (2 to 8 h) throughout an incubation period of 72 to 80 h. The *P/E* curve of the compiled data set was described with the equation of Webb et al. (1974). The estimated parameters are the capacity of net community production NCP_{max} = 0.67 mmol O_2 m^{-2} h^{-1} (with 95 % confidence interval [CI] = 0.23 to 1.09), the initial slope α = 0.12 mmol O_2 m^{-2} h^{-1} (µmol photons m^{-2} s^{-1})$^{-1}$ (with 95 % CI = 0.06 to 0.18) and the dark community consumption DCC = −1.35 mmol O_2 m^{-2} h^{-1} (with 95 % CI = −1.70 to −1.00). Accordingly, the capacity of gross community production (GCP) is GCP_{max} = 2.01 mmol O_2 m^{-2} h^{-1}. NCP is positive at PFDs >19 µmol photons m^{-2} s^{-1}. Shown are the estimated *P/E* curve (solid line) and the upper and lower 95 % confidence band (dashed lines)

benthic chamber and 3 additional from the adjacent area) with Plexiglas™ sediment tubes (internal diameter 50 mm, 250 mm length; Fig. 1). They were transported to the laboratory under dark conditions and kept in a cool room at 2°C until further biomass determination, which was conducted as quickly as possible (within 4 h) after sampling.

Biomass analyses

All cores (n = 6; Fig. 1) were sectioned horizontally immediately after the *in situ* measurements. Each top 5 mm slice was weighed and homogenised manually before subsamples were taken. Subsamples were weighed again for chlorophyll *a* and organic content analysis (POC: particulate organic carbon, PON: particulate organic nitrogen).

Chlorophyll *a* was extracted in subsamples of ~2 to 4 g fresh biomass in 5 ml 90% acetone (v/v) for 24 h in the dark at 4 to 5°C according to Jeffrey & Humphrey (1975). The samples were then centrifuged for 5 min at 7200 g and 5°C, supernatants were collected and absorbance was determined. Pellets were re-extracted twice according to this procedure to improve the extraction efficiency by resuspending in 2.5 ml 90% acetone.

Total organic carbon (TOC) and total nitrogen (TN) contents were determined in dried samples (6 h at 105°C). Samples of 50 to 100 mg dry biomass were combusted in an elementar analyser (Vario EL, Elementar GmbH) according to Verardo et al. (1990) following acidification of the samples in silver cups with 50 to 100 µl 10% HCl (v/v) to remove inorganic carbonates. The dry and carbonate free samples were squeezed airtight in tin foil as pellets and then measured.

Patchiness of biomass and community production

We first investigated the impact of the stations (i.e. NAT, LON, BRL) and water depths (i.e. shallow, intermediate, deep) on microphytobenthos biomass estimated as chlorophyll *a* concentrations (mg chl *a* m^{-2}) and TOC (mg g^{-1}). As the 3 × 3 fixed factorial design was unbalanced with unequal replication (n = 3 at BRL-deep, n = 6 otherwise) and missing observations (at LON-deep), we fit a simple cell means ANOVA model according to Quinn & Keough (2002) and Logan (2010). The means model treats all replicated factor-level combinations as levels of a single factor in a single-factor ANOVA (Type III sums of squares). We tested relevant and estimable contrasts based on cell means, i.e. only those not relying on the missing cell.

Additionally, a principal component analysis (PCA; Legendre & Legendre 2012) was performed to identify structures in the multidimensional data set of all samples with respect to 6 descriptor variables of sediment assemblages: chl *a* concentration (mg chl *a* m^{-2}), water content (%), TOC (mg g^{-1}), C:N ratio (mol mol^{-1}), DCC (mmol O_2 m^{-2} h^{-1}) and NCP (mmol O_2 m^{-2} h^{-1}). PCA is an ordination method and aims to represent the data along a reduced number of new theoretical variables — the principal components (PCs). To illustrate the relative positions of the samples along the descriptor variables, 2-dimensional biplots of the first 2 PCs were drawn. In the distance biplot (scaling 1), distances among sites are approximations of their Euclidean distances in the multidimensional space; projecting a sample at a right angle on a descriptor variable approximates the position of this sample along that descriptor variable. The correlation biplot (scaling 2) is inadequate to interpret distance relationships among samples. However, the length of the projection of the descriptor variables is an approximation of its standard deviation and the angles between descriptor variables reflect their correlations. The statistical analyses were performed with the software R 2.15.1 for statistical computing (R Core Team 2013). PCAs were calculated with the R-package 'vegan' (Oksanen et al. 2012). All variables were standardised to account for the different measurement scales of the 6 parameters.

Modelling seasonal and regional NCP rates

We applied the numerical model of Walsby (1997) to estimate hourly, depth-resolved and depth-integrated NCP rates of microphytobenthos in Kongsfjorden along the water depth gradient between 3 and 30 m with a spatial resolution of 1 m. The upper 3 m were excluded because of the tidal range (~2 m). However, instead of using the spreadsheet version published by Walsby (1997), we wrote a Matlab script (Matlab R2010b, MathWorks) for NCP rates during the Arctic spring and summer (1 April until 31 August 2008). The Walsby numerical model estimates NCP rates as a function of photosynthetic capability (i.e. the parameters of the regional *P*/*E* curve: NCP_{max}, α and DCC obtained from all 55 *in situ* O_2 exchange rates measured in benthic chambers; Fig. 3) and relevant abiotic parameters (i.e. underwater PAR and water temperature). For the

days of 2008, global solar radiation (305 to 2800 nm, 2 m above ground, measurements with 1 Hz sampling rate, processing of hourly data, CM11 Pyranometer with global radiation sensor, Kipp & Zonen, Delft) and wind speed (10 m above ground, hourly data, wind meter with Combined Wind Sensor Classic, Adolf Thies GmbH and Co. KG) were obtained from the Climate Science division of the Alfred Wegener Institute (courtesy of S. Debatin). Global solar radiation data in W m^{-2} were converted to PFDs of PAR (400 to 700 nm) by applying a globally measured mean ratio of PAR to global solar radiation of 0.48 (Table 2 in Tsubo & Walker 2005) and by converting 1 W m^{-2} of PAR to 4.6 µmol photons m^{-2} s^{-1} (Morel & Smith 1974). Satellite-derived sea surface temperatures (SSTs) produced by the AMSR-E (Advanced Microwave Scanning Radiometer) were used (data available at www.remss.com). SST data mapped to a 0.25° grid were spatially averaged over 75.5 to 79.5° N and 8.0 to 12.0° E, i.e. the area off the west coast of Svalbard and covering the Westspitsbergen Current. Three-day moving averages were chosen to minimise data gaps caused by cloud cover or high wind speed. The Walsby numerical model accounts for light reflection at the water surface, which depends on the solar angle and roughening of the sea surface by wind. To calculate vertical light attenuation, we chose a mean K_d value of 0.2 m^{-1} (measured at 3 stations every 10 min during all measurement campaigns in June 2008; SD ± 0.04). The model also includes the temperature dependence of DCC and NCP according to van't Hoff's rule (Q_{10} value). As we did not determine short-term temperature effects of NCP, we adopted Q_{10} values from Hancke & Glud (2004) that were determined in a diatom-dominated benthic community in the Arctic Adventfjord (Svalbard, Norway). The authors determined Q_{10} values of 2.4 in darkness (n = 5) and 1.5 in light (n = 2) with the help of total oxygen exchange rates at 5 different temperatures (–2 to 12°C). Due to the limited range of data for Arctic microphytobenthos, we used Q_{10} = 2.4 for DCC and Q_{10} = 1.5 for GCP to simulate the temperature dependence of NCP. Primary production along the water depth gradient was estimated for 2 'extreme' hydrodynamic conditions (maximum and minimum) for an Arctic fjord: (1) a stable stratification of the water column due to freshwater discharge from melting snow layers and glaciers occurring during the summer months; and (2) a fully mixed water column. We considered different temperature gradients but not different light transmittance in these 2 scenarios. The temperature gradients were set according to the temperature profiles measured by Hanelt et al. (2001) in Kongsfjorden. In the stratified water column, temperature was constant in the upper 3 to 5 m and then suddenly decreased to 0.1°C. In the mixed water column, temperature linearly decreased from the SST at 3 m to 0.5°C at 30 m. Additionally, we analysed the quantitative effect of the proposed increase in SST of 2°C on microphytobenthic primary production according to predictions for the summer warming until 2100 in Kongsfjorden (MacDonald 2010).

To build confidence in the model, we also performed a sensitivity analysis by studying the uncertainties of the associated model parameters. We calculated NCP for the lower and upper 95% confidence band of the P/E curve and the mean Q_{10} values given by Hancke & Glud (2004). To include effects of uncertainty of the Q_{10} value, as no uncertainties were given by Hancke & Glud (2004), we also calculated NCP for the 34.1% lower and 34.1% higher estimates of the Q_{10} values and the mean P/E curve. The lowest Q_{10} estimates were 1.6 in darkness and 1.0 in light. The highest Q_{10} estimates were 3.2 in darkness and 2.0 in light.

Finally, we present daily, water depth-resolved rates of NCP (mmol O_2 m^{-2} d^{-1}). To determine rates for the entire Kongsfjorden, we needed to calculate the total shore area. The total shoreline length of Kongsfjorden is 106.92 km (coastline without islands: 37.52 km). Thus, the total shore area of Kongsfjorden down to 30 m water depth is 3.21 km^2. Woelfel et al. (2009a) determined bottom characteristics by echo sounding 37.41 km, down to 30 m water depth, with a spatial resolution of 0.3 to 0.9 m (according to depth) × 0.08 m. Thus, 1.12 km^2 were surveyed and of this investigated area, only 0.7 km^2 (32%) was covered by sandy and muddy sites. Consequently, we extrapolated that 1.03 km^2 (32% of the total shore area) of Kongsfjorden is suitable for benthic microalgae growth. We calculated regional, water depth-integrated NCP rates for the entire Kongsfjorden (×10^3 mol O_2 d^{-1}) between 3 and 30 m water depth.

RESULTS

Environmental conditions

In June 2008, the salinity of the surface water (≤1 m) of Kongsfjorden ranged between 33 and 35 PSU, while water temperature (3 to 11 m water depth) varied between 2.7 and 4.5°C (minimum and maximum values, n = 55; data not shown). The dominant sediment type at Stns NAT and BRL was middle-grained, well-sorted sand with modal particle

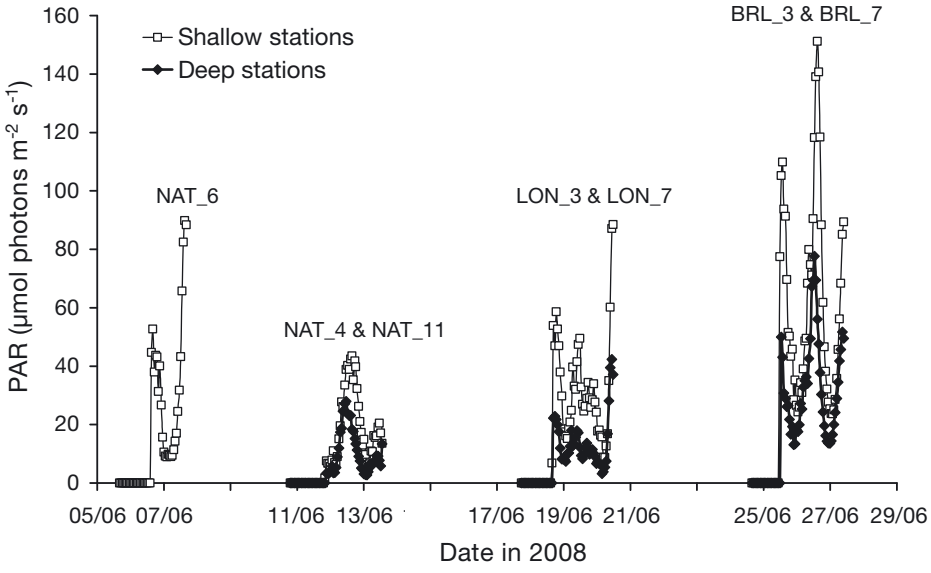

Fig. 4. Underwater photon fluence rates (µmol photons m^{-2} s^{-1}) during each experimental period at the 3 stations Nansenbay (NAT), London (LON) and Brandal (BRL); numbers after the stations refer to the water depth (m). The signal was recorded every 15 to 20 s, and hourly means were processed

sizes between 0.2 and 0.3 mm. The sediment at Stn LON was composed of slightly coarser, middle-grained sand with modal particle sizes between 0.3 and 0.4 mm (data shown in Woelfel et al. 2009a).

Although snow melting increased in the middle of June, the water transparency at the incubation sites was continuously high with low K_d values: between 0.02 and 0.21 m^{-1} at Stn NAT, between 0.19 and 0.27 m^{-1} at Stn LON and between 0.09 and 0.19 m^{-1} at Stn BRL. Accordingly, underwater irradiance of PAR did not considerably differ between sites and depths (Fig. 4).

In situ primary production June 2008

In situ DCC rates were high over the whole field period (June 2008) and mean values ranged between −1.7 and −0.45 mmol O_2 m^{-2} h^{-1}, indicating high heterotrophic activity in the sediment (Fig. 5). This strong oxygen consumption was in accordance with very low NCP rates of maximal 0.6 mmol O_2 m^{-2} h^{-1} (corresponding to 0.8 mg O_2 mg^{-1} chl *a* h^{-1}). NCP was negative at 4 of the 7 investigated sites. Differences in GCP rates, i.e. the sum of DCC and NCP rates, between water depths were generally lacking. Only minor differences were found at Stn BRL, where high GCP rates of 0.8 and 2.3 mmol O_2 m^{-2} h^{-1} (NCP rates: 0.8 and 0.4 mg O_2 mg^{-1} chl *a* h^{-1}) were measured at 3 and 7 m water depth, respectively.

Heterogeneity between and within sites

All 4 descriptor variables of sediments (chl *a*, water content = proxy for grain size, TOC, C:N ratio) that were determined in 42 samples showed a high variability, indicating that Kongsfjorden's benthic ecosystem is very heterogeneous (Table 1, Fig. 6). This is true between sites that are a few kilometres apart

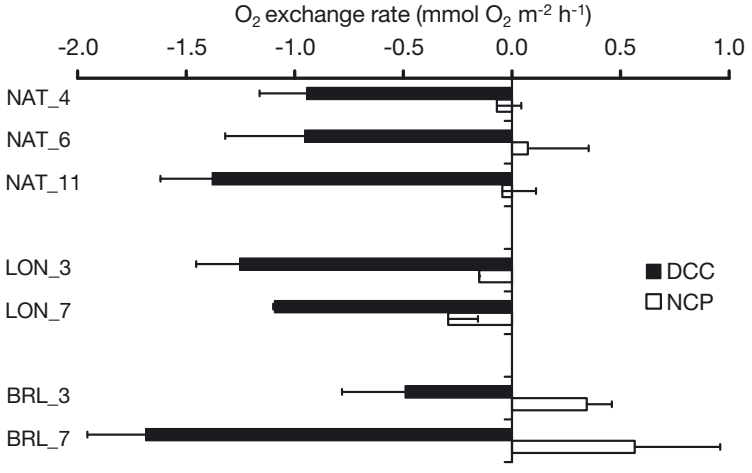

Fig. 5. Total rates of *in situ* dark community consumption (DCC) and net community production (NCP) measured as oxygen exchange rates over the whole 72 to 80 h incubation period (mmol O_2 m^{-2} h^{-1}) at the 3 stations Nansenbay (NAT), London (LON) and Brandal (BRL) and different water depths. Numbers after the stations refer to the sampled water depth (m). Shown are means and standard deviations (n = 3). Production measurements at LON_3 was n = 1 due to technical problems

Table 1. Sediment characteristics at the 3 sampling sites Nansenbay (NAT), London (LON) and Brandal (BRL) in Kongsfjorden at different water depths (June 2008). Shown is the range (minimum and maximum) of the data (n = 6; BRL at 15 m: n = 3)

Station	Depth (m)	Water content (%)	C:N ratio (mol mol^{-1})
NAT	4	23–29	16–31
NAT	6	28–31	28–40
NAT	11	26–36	27–31
BRL	3	22–24	46–93
BRL	7	26–34	25–49
BRL	15	23–27	26–67
LON	3	12–22	27–78
LON	7	14–26	18–76

and along a small depth gradient of a few meters, as well as within sites at a specific depth level. Biomass ranged in all samples between 10 and 97 mg chl *a* m^{-2}. Chl *a* concentrations of replicated samples were in some cases very similar (e.g. BRL at 3 m: 10 to 12 mg chl *a* m^{-2}), but differed at other stations (e.g. LON at 7 m: 12 to 62 mg chl *a* m^{-2}). Similarly, organic carbon content showed a high variability between 0.5 and 5.6 mg g^{-1} dry weight. This high variability in both chl *a* concentration and TOC is also clear from the interaction boxplots (Fig. 6). Statistical analysis revealed almost no significant differences in microphytobenthos biomass, between both stations and water depths (Table 2). The picture is slightly different for the TOC content of the sediment. TOC was higher in Stn NAT than in Stn BRL when averaged over all 3 depths. As a monotonic dependence between water depth and microphytobenthic biomass was lacking, differences in hydrological conditions rather than underwater light determine microphytobenthos distribution patterns.

PCA was performed to summarise the heterogeneous and patchy distribution of the sediment characteristics (Table 1, Fig. 6) together with the production measurements (DCC, NCP; Fig. 5). Biplots illustrate the relative position of the stations along the 6 descriptor variables of sediment assemblages (chl *a*, water content, TOC, C:N ratio, DCC and NCP) and with respect to PC1 and PC2 (Fig. 7). The PCA explained 63% of the variability in the data on the first 2 PC axes. Water content, DCC, C:N ratio and chl *a* have the highest correlation with PC1. TOC and NCP have the highest correlation with PC2. To illustrate systematic differences between samples with respect to the station (NAT, BRL, LON) and to the depth (shallow, intermediate, deep), we assigned different symbols for each station and different shading for the depth levels. It is important to keep in mind that PCA is not a statistical test; it aims at representing major features of the data along a reduced number of axes.

We were not able to identify any clear patterns between sampling sites and along the descriptor variables (distance biplot, Fig. 7A). Most samples taken at Stn NAT (circles) group at the origin of the biplot, i.e. have average values of most parameters. The samples taken at Stn BRL (triangles) have higher chl *a* concentrations but lower DCC rates at 7 m than at 3 m. Chl *a* and NCP are positively correlated and both variables are negatively correlated with DCC (correlation biplot, Fig. 7B). The variance of the 6 descriptor variables is similar, as there is little difference in length of the arrows.

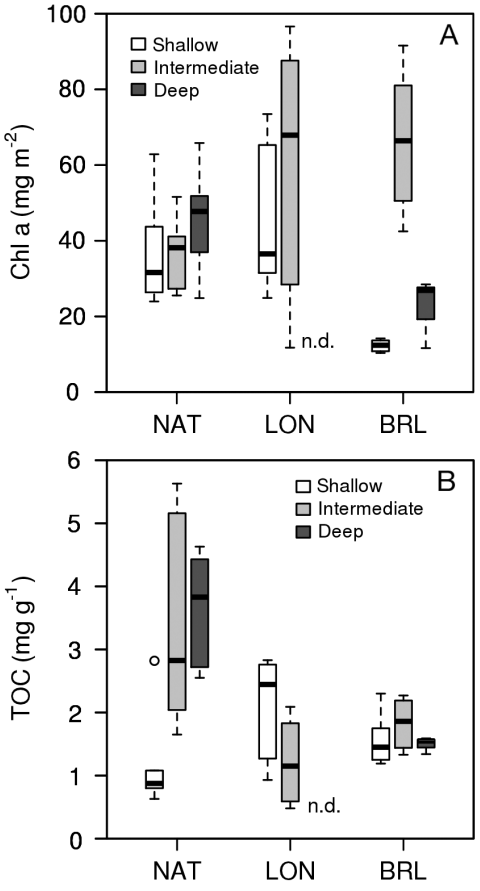

Fig. 6. Interaction plot of (A) chlorophyll *a* concentration (mg chl *a* m^{-2}) and (B) total organic carbon (mg TOC g^{-1}). Results of cell means ANOVA model are shown in Table 2. Shallow water depth means: 4 m for Nansenbay (NAT) and 3 m for Brandal (BRL) and London (LON); intermediate water depth: 6 m for NAT and 7 m for LON and BRL; deep water depth: 11 m for NAT and 15 m for BRL. n.d. = no data. Boxes show the range between the 25th and 75th percentiles, the line within each box indicates the median, and the whiskers extend to 1.5 times the interquartile range from the box. Data points located outside the whiskers are defined as outliers

Table 2. Cell means ANOVA model according to Quinn & Keough (2002) and Logan (2010) with relevant tests for the main effects of 'station' and 'water depth' and their interaction. (a) Unbalanced 3 × 3 fixed factorial design with unequal replication (n = 3 at BRL-deep, n = 6 otherwise) and a single missing cell (nd; at LON-deep). (b) ANOVA results for chlorophyll *a* concentration (mg chl *a* m^{-2}) and total organic carbon (TOC, mg g^{-1}). Shallow water depth means: 4 m for Nansenbay (NAT) and 3 m for Brandal (BRL) and London (LON); intermediate water depth: 6 m for NAT and 7 m for LON and BRL; deep water depth: 11 m for NAT and 15 m for BRL. Significance levels: $^{*}p < 0.05$, $^{**}p < 0.01$, $^{***}p < 0.001$

(a) Factorial design

	NAT	LON	BRL
Shallow	n = 6	n = 6	n = 6
Intermediate	n = 6	n = 6	n = 6
Deep	n = 6	nd	n = 3

(b) ANOVA results

	Chlorophyll *a* concentration					Total organic carbon				
Source	df	SS	MS	*F*	p	df	SS	MS	*F*	p
Cells:	7	12436	1776.6	5.519	<0.001***	7	37.19	5.313	6.836	<0.001***
Station:										
NAT vs. BRL marginal means	1	1104	1104.2	3.43	0.072	1	9.43	9.43	12.14	0.001**
NAT vs. LON for shallow and intermediate depth	1	1749	1748.7	5.433	0.025*	1	2.67	2.67	3.43	0.072
BRL vs. LON for shallow and intermediate depth	1	377	377.1	1.172	0.286	1	4.54	4.54	5.84	0.021*
Depth:										
Shallow vs. intermediate marginal means	1	705	705.5	2.19	0.147	1	2.42	2.42	3.115	0.086
Shallow vs. deep for NAT and BRL	1	147	147.2	0.46	0.503	1	11.01	11.01	14.17	<0.001***
Intermediate vs. deep for NAT and BRL	1	369	369	1.15	0.291	1	5.14	5.14	6.61	0.014*
Station × depth:										
NAT vs. BRL for intermediate and deep depth	1	3376	3376	10.49	0.003**	1	1.84	1.84	2.37	0.132
NAT vs. BRL for shallow and deep depth	1	688	688	2.14	0.152	1	10.23	10.23	13.17	<0.001***
LON vs. BRL for shallow and intermediate depth	1	282	282	0.876	0.355	1	5.08	5.08	6.54	0.015*
Residual:	37	11910	321.9			37	28.76	0.777		

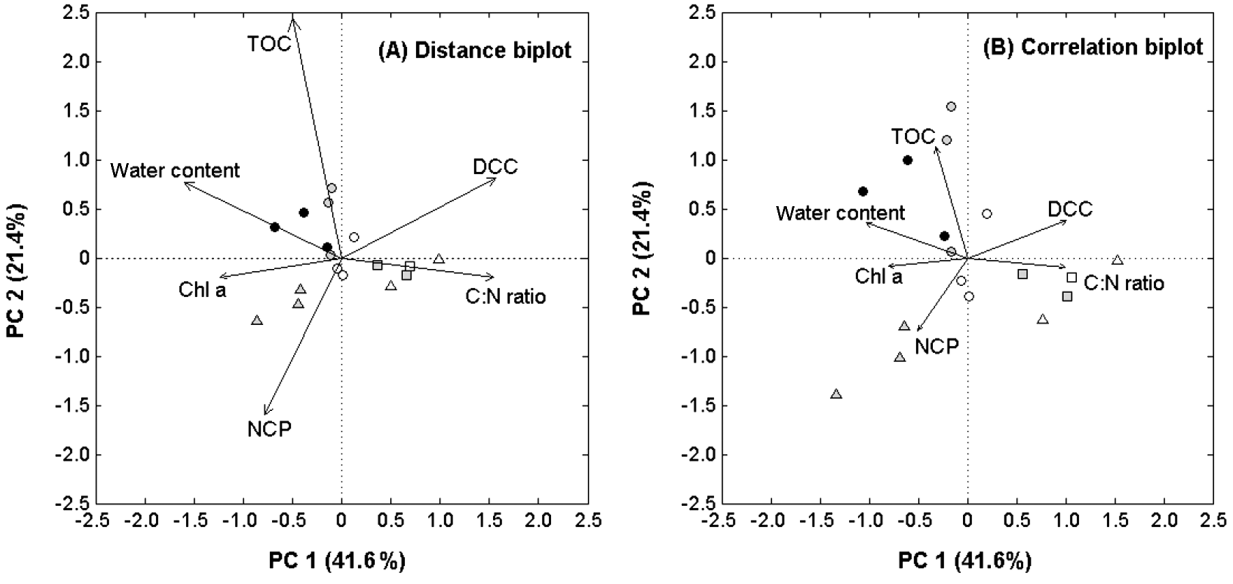

Fig. 7. (A) Distance biplot and (B) correlation biplot of the first 2 principal components of a principal component analysis (PCA) illustrating the relative positions of 17 samples along 6 variables of sediment assemblages to describe patterns within and between sampling sites: chlorophyll *a* content (chl *a*, mg m^{-2}), water content (% dry weight), total organic carbon (TOC, mg g^{-1}), C:N ratio (mol mol^{-1}), DCC (mmol O_2 m^{-2} h^{-1}) and NCP (mmol O_2 m^{-2} h^{-1}). Symbols represent the 3 stations (Nansenbay: circles, London: squares, Brandal: triangles) and shading represents the depth levels (white: shallow 3 to 4 m, grey: intermediate 6 to 7 m, black: deep 11 m). PC1 explains 41.6 % and PC2 21.4 % of the variance in the data set

Modelled primary production for the Arctic spring and summer 2008 and predicted future changes

A mean regional *P/E* curve with a 95% confidence band was compiled from all 55 *in situ* NCP rates and the respective mean underwater irradiance of each measurement interval (Fig. 3). The derived parameters and the respective 95% confidence intervals (CI) are NCP_{max} = 0.67 mmol O_2 m^{-2} h^{-1} (with 95% CI = 0.23 to 1.09), the initial slope α = 0.12 mmol O_2 m^{-2} h^{-1} (µmol photons m^{-2} s^{-1})$^{-1}$ (with 95% CI = 0.06 to 0.18) and DCC = −1.35 mmol O_2 m^{-2} h^{-1} (with 95% CI = −1.70 to −1.00). Accordingly, the capacity of GCP is GCP_{max} = 2.01 mmol O_2 m^{-2} h^{-1}. The light saturation point E_k is defined as the intersection between the initial linear slope and the maximum rate. According to the fitted curve, the intersection of the mean *P/E* curve is at 17 µmol photons m^{-2} s^{-1}. Due to the large uncertainty of the broad confidence band of the curve (computed in Fig. 3), the range of the light compensation point overlaps with this mean E_k value. Corresponding to the lower and upper confidence band, E_k ranges between 14 and 22 µmol photons m^{-2} s^{-1}, indicating that NCP is saturated at very low underwater irradiances.

The parameters of the regional *P/E* curve (NCP_{max}, α, DCC) were implemented into the numerical primary production model of Walsby (1997) to estimate daily rates of primary production in Kongsfjorden for the Arctic summer 2008 for a water depth gradient between 3 and 30 m. During June 2008, PAR at the sea surface ranged between 39 and 486 µmol photons m^{-2} s^{-1} at polar midnight and 273 and 1406 µmol photons m^{-2} s^{-1} at noon (Fig. 8A). The PAR at the sea surface for the Arctic spring and summer seasons (1 April until 31 August 2008) ranged between 4 and 486 µmol

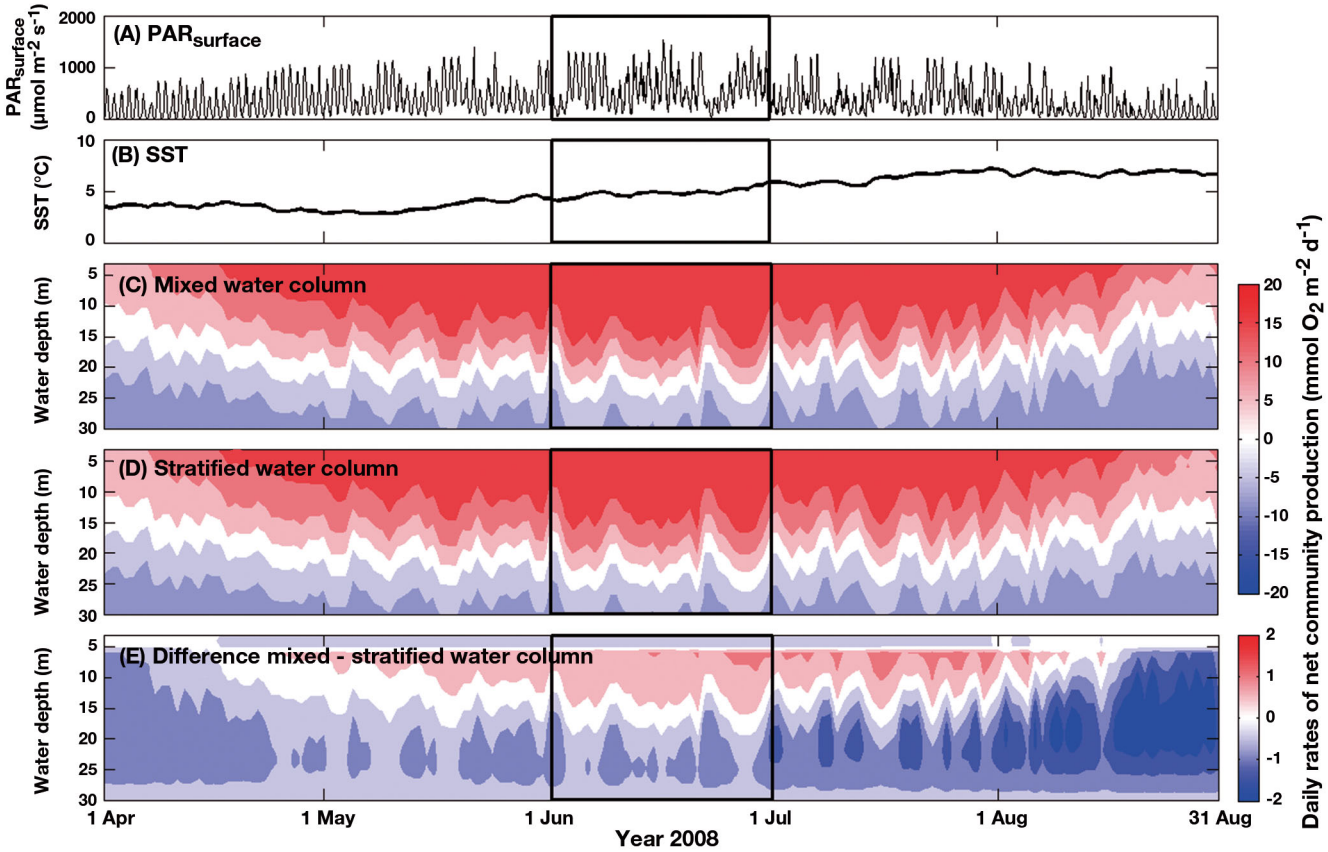

Fig. 8. Water depth-resolved, daily net community production (NCP) rates between 3 and 30 m water depth in Kongsfjorden were estimated with the numerical model of Walsby (1997) for the 2008 Arctic spring and summer seasons (1 April until 31 August). The experimental period of this study (June 2008) is highlighted. The *P/E* curve parameters derived from the compiled *in situ* data set were used (Fig. 3). NCP depends on (A) incident photosynthetically active radiation as estimated from hourly global radiation data and (B) the satellite-derived daily sea surface temperatures (SST). NCP was calculated for 2 mixing scenarios according to the measured temperature profiles of Hanelt et al. (2001), i.e. a well mixed (C) and a stratified (D) water column; the difference between the 2 scenarios is also shown (E). The colour bar depicts NCP rates between −20 and +20 mmol O_2 m^{-2} d^{-1} for the 2 mixing scenarios (C,D). The difference between the 2 scenarios amounts to maximal 10% of the predicted NCP rates and the colour bar depicts daily NCP rates between −2 and +2 mmol O_2 m^{-2} d^{-1} (E)

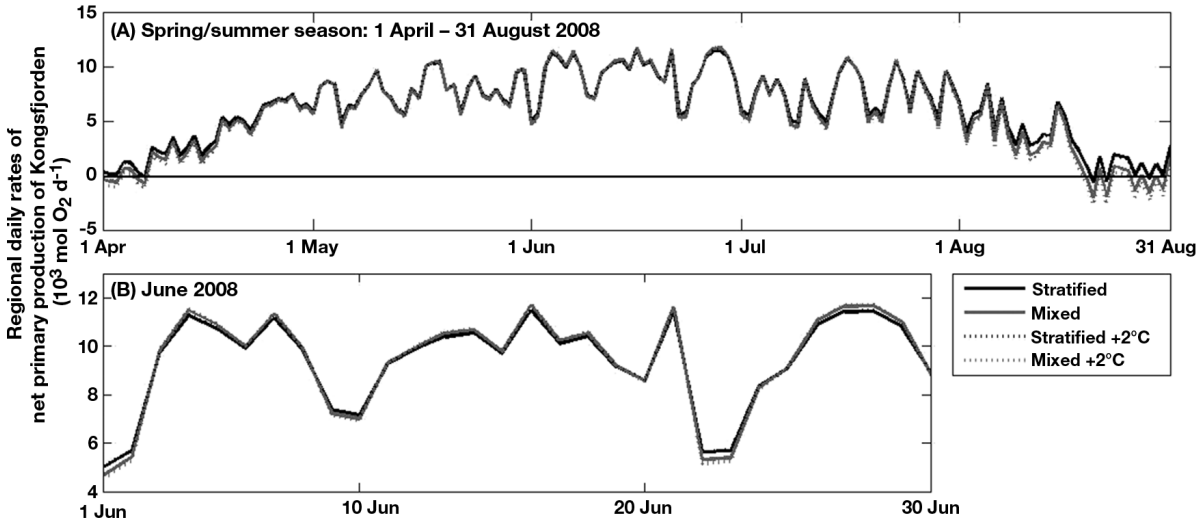

Fig. 9. Regional, depth-integrated daily rates of net primary production (NCP) of Kongsfjorden (×10^3 mol O_2 d^{-1}) were estimated with the numerical model of Walsby (1997). NCP rates were integrated between 3 and 30 m water depth and were extrapolated to all the Kongsfjorden sandy and muddy sites (32% of the 106.9 km coastline according to Woelfel et al. 2010). NCP rates are shown for (A) the 2008 Arctic spring and summer seasons (1 April until 31 August) and (B) the experimental period of the present study (June 2008)

photons m^{-2} s^{-1} at polar midnight and 107 and 1406 µmol photons m^{-2} s^{-1} at noon (April–August, Fig. 8A). Satellite-derived sea surface temperatures were between 4.1 and 5.6°C in June 2008 and between 2.8 and 7.2°C for the Arctic summer period (Fig. 8B).

Based on PAR and temperature data, the mean regional *P/E* curve and the mean Q_{10} values given by Hancke & Glud (2004), the model estimated positive NCP rates at shallow water depths <10 m for the entire period (1 April until 31 August 2008) and for both hydrographic scenarios (Fig. 8C,D). Rates ranged between 15 and 18 mmol O_2 m^{-2} d^{-1} in summer (June to July) at shallow depths. However, independent of the water column scenario, NCP rates were never positive below 25 m water depth. The 2 hydrographical scenarios, i.e. the 2 vertical temperature gradients, differed only slightly by a maximum of 10% (Fig. 8e). The mixed water column (between 5 and 15 m water depth) yielded higher NCP rates in June and July (maximal 1 mmol O_2 m^{-2} d^{-1}) compared with the stratified water column. The stratified scenario yielded higher NCP rates at lower water depth (maximal 2 mmol O_2 m^{-2} d^{-1}).

As expected from the depth-resolved data (Fig. 8), water depth-integrated, daily NCP rates for the entire Kongsfjorden were very similar for both hydrographical scenarios and ranged between -2×10^3 and $+12 \times 10^3$ mol O_2 d^{-1} during Arctic spring and summer 2008 (Fig. 9A). NCP was negative only at the very beginning of April and during the last third of August. Accordingly, the respective rates for the field period June 2008 were always positive and ranged between 5×10^3 and 12×10^3 mol O_2 d^{-1} (Fig. 9B). Additionally, the predicted increase in SST by 2°C caused only a very minor increase in NCP by a maximum of 0.04×10^3 and 0.07×10^3 mol O_2 d^{-1} for the 2 hydrographical conditions.

The regional, depth- and time-integrated NCP rate of Kongsfjorden for the Arctic spring and summer seasons is positive, pointing to a net autotrophic coastal ecosystem (Table 3). The numerical model estimated an oxygen evolution of 9 t (corresponding to a carbon fixation of 3 t) for June 2008 and 30 t O_2 (corresponding to 11 t C) for the entire spring and summer seasons. Based on the uncertainties of the *P/E* curve, i.e. calculations for the lower and upper 95% confidence band of the *P/E* curve, NCP varied by 11 to 19% and rates extended between 8 and 10 t O_2. Including uncertainties of the Q_{10} values caused a much higher variability between 24 and 76%. NCP rates ranged between 6 and 16 t O_2 in these cases. Notably, all scenarios yielded positive NCP rates.

DISCUSSION

Marine benthic primary production in the Arctic takes place at permanently low temperatures (–1.5 to 1.8°C), except in some shallow-water areas where temperatures can reach higher values during the summer open-water period (Krause-Jensen et al. 2007). Most microphytobenthic primary production

Table 3. Regional net community production (NCP; in tonnes of O_2 and C) of Kongsfjorden estimated with the numerical model of Walsby (1997) for June 2008 and the spring and summer seasons (1 April to 31 August 2008). Depth-integrated NCP rates between 3 and 30 m water depth were extrapolated to all the Kongsfjorden sandy and muddy sites (32% of the 106.9 km coastline according to Woelfel et al. 2010). Seasonal data were derived from incident photosynthetically active radiation as estimated from hourly global radiation data and satellite-derived daily sea surface temperatures from 1 April to 31 August 2008. Presented NCP rates are based on the estimated parameters of the mean *P/E* curve and Q_{10} values given by Hancke & Glud 2004. Q_{10} values for photosynthesis in light and dark respiration differ (see total oxygen exchange in Table 3 in Hancke & Glud 2004; darkness: Q_{10} = 2.4; light: Q_{10} = 1.5). To quantify effects of uncertainty in the estimates of the *P/E* curve, NCP of Kongsfjorden was also calculated for the lower and upper 95% confidence band of the *P/E* curve and the mean Q_{10} values. To quantify effects of uncertainty in the estimates of the *P/E* curve Q_{10} values, NCP was also calculated for lowest (darkness: Q_{10} = 1.6; light: Q_{10} = 1.0) and highest (darkness: Q_{10} = 3.2; light: Q_{10} = 2.0) estimates of the Q_{10} values at the mean *P/E* curve. Relative differences to the mean estimates (in bold) are given in parentheses

Scenario water column and time period	NCP regional rates									
	Mean *P/E* curve, mean Q_{10} values		Lowest *P/E* curve, mean Q_{10} values		Highest *P/E* curve, mean Q_{10} values		Mean *P/E* curve, lowest Q_{10} values		Mean *P/E* curve, highest Q_{10} values	
	O_2 (t)	C (t)	O_2 (t)	C (t)	O_2 (t)	C (t)	O_2 (t)	C (t)	O_2 (t)	C (t)
June 2008										
Stratified	**8.99**	**3.37**	7.97 (–11%)	2.99	10.13 (+13%)	3.80	15.82 (+76%)	5.93	6.04 (–33%)	2.26
Mixed	**9.03**	**3.38**	7.66 (–15%)	2.87	10.52 (+17%)	3.94	14.19 (+57%)	5.32	6.55 (–28%)	2.46
Stratified +2°C	**9.00** (+0.2%)	**3.38**	7.92 (–12%)	2.97	10.21 (+13%)	3.83	15.61 (+73%)	5.85	6.14 (–32%)	2.30
Mixed +2°C	**9.01** (–0.1%)	**3.38**	7.41 (–18%)	2.78	10.74 (+19%)	4.03	13.29 (+47%)	4.98	6.84 (–24%)	2.57
Spring and summer seasons (April to August 2008)										
Stratified	**30.55**	**11.46**	24.93 (–18%)	9.35	36.66 (+20%)	13.75	52.98 (+73%)	19.87	20.79 (–32%)	7.80
Mixed	**29.06**	**10.90**	21.58 (–26%)	8.09	37.03 (+27%)	13.89	44.30 (+52%)	16.61	21.54 (–26%)	8.08
Stratified +2°C	**30.53** (–0.1%)	**11.45**	24.58 (–20%)	9.22	36.97 (+21%)	13.86	51.90 (+70%)	19.46	21.17 (–31%)	7.94
Mixed +2°C	**28.22** (–2.9%)	**10.58**	19.55 (–31%)	7.33	37.38 (+32%)	14.02	39.67 (+41%)	14.88	22.10 (–22%)	8.29

measurements have been carried out on tidal or non-tidal shallow-water habitats <5 m (e.g. reviewed in Cahoon 1999). However, similar studies along larger depth gradients between 5 and 100 m and specifically in polar regions are very rare (e.g. Wulff et al. 2005). This may be explained by the methodological difficulties of *in situ* measurements in general, and specifically in polar regions, as well as by the limited working range of research vessels in shallow-water habitats. A number of areal and temporal estimates have been made worldwide based on inter- and extrapolation, but a high number of undersampled and unsampled coastal areas in polar regions still exist (Sakshaug 2004).

Furthermore, microphytobenthic biomass is known to show high spatial heterogeneity and patchiness at different scales from millimetres to kilometres (Brotas & Plante-Cuny 1998, Jesus et al. 2005). Our data on sediment characteristics fully support these results. Both phytobenthos biomass and TOC showed a high variability within sites, even at a specific depth level (Figs. 6 & 7, Table 2). Patchiness and underlying controlling factors, such as substrata types, hydrology and species-specific physiological acclimation, complicate the upscaling of point measurements to regional estimates. Additionally, these factors complicate the application of primary production models. Spilmont et al. (2011) concluded that most depth-integrated estimates of microphytobenthos production are likely to be strongly biased by ±40%.

We specifically adjusted our *in situ* approach to counteract the effects of microphytobenthos patchiness as much as possible. The benthic incubation chambers with a diameter of 140 mm integrate gross production on a spatial scale that is more adequate than 'point' microsensor measurements. Planar oxygen sensor spots glued inside the benthic chambers allow determination of oxygen evolution without regular subsampling or destructing sediments under different (and Arctic) temperatures or irradiation levels (*P/E* curves). Replicate chambers (*in situ* up to 12 m water depth) can easily be incubated and analysed in parallel. As the sensor spots do not consume O_2 themselves (in contrast to Clark electrodes), online measurements of very low oxygen concentrations are possible over days (Woelfel et al. 2009b). Furthermore, and in contrast to microprofile approaches, associated biomass parameters are available to which microphytobenthic production could be normalised (i.e. chl *a* concentration per sediment area, volume or mass). Thus, we could minimise a number of biases (e.g. patchiness) with our *in situ*

benthic chamber set-up, and hence, the aerial community production rates are quite reliable.

The *in situ* measurements yielded mean GCP rates of ~0.8 to 2.3 mmol O_2 m^{-2} h^{-1} (10 to 26 mg C m^{-2} h^{-1}), which are comparable to other polar regions, e.g. Signy Island, Antarctica, in 8 m water depth, where 13 to 29 mg C m^{-2} h^{-1} were measured in coarse sandy sediments (Gilbert 1991). In our study, chl *a* contents (14 to 63 mg chl *a* m^{-2}) and GCP rates were determined, and are similar to those on sandy sediments of temperate waters, despite much lower Arctic water temperatures (cf. Table 6 in Woelfel et al. 2009a, cf. Table 3 in Woelfel et al. 2010). Therefore, photosynthesis of Arctic microphytobenthos seems to be well adapted to polar conditions.

DCC as a summand of GCP was not directly related to the chl *a* concentration (Fig. 7). In contrast to pelagic studies, the large spatial variability of organic matter debris, bacteria, zoo- and microphytobenthos, and consequently all biogeochemical processes, restrict the data interpretation. Thus, we decided to calculate the GCP, NCP and DCC rates as aerial community oxygen exchange rates, which is common in sediment studies (i.e. in the review of Glud et al. 2009), and not as rates normalised to phototrophic biomass. Furthermore, we are convinced that the separate presentation of NCP and DCC allows a more detailed discussion of sediment ecology. Our data indicated that low *in situ* NCP rates were determined not because of low photosynthetic rates of benthic microalgae but rather because of the very high (2- to 3-fold higher) oxygen consumption rates of the entire benthic community (Fig. 5). High oxygen consumption rates in sediments are very common and are mainly attributed to high hetero- and autotrophic activities of dense microbial and zoobenthic communities. It is likely that in the protected bay of Kongsfjorden more organic material is deposited, thus enhancing these activities. The respiratory activity of dense communities, such as meiozoobenthos communities, can be more stimulated in light than in darkness (i.e. Hancke & Glud 2004, Woelfel et al. 2010). Additionally, the abiotic chemical oxygen demand of reduced inorganic compounds (such as iron or sulphur compounds) has only inadequately been investigated in sediments (Schippers & Jørgensen 2001, Jørgensen & Nelson 2004). Because all of these processes were not quantified separately in this study, we cannot exclude any potential impact on NCP measurements.

Although the use of benthic chambers in combination with oxygen sensor spots provides an excellent approach for *in situ* community production and consumption measurements, it exhibits only a limited insight into the vertical distribution and activity of sediment dwelling organisms, e.g. vertical migrating benthic diatoms (Kühl et al. 1996) or bacterial degradation. The quantification of these microscale processes with microelectrode profiling (either optical or Clark electrodes) or image-guided methods (e.g. optode foils, PAM fluorometry) would add valuable information and are recommended for future studies.

Both microphytobenthos biomass and NCP rates neither decreased with increasing water depth nor showed any specific pattern with water depth (Figs. 5–7). As already shown in Woelfel et al. (2009a, 2010), no key abiotic factor explaining different biomass at the different sandy stations in Kongsfjorden could be identified, although sediment characteristics, nutrient and light availability, salinity and temperature were tested. We suggest that hydrodynamic conditions primarily limit local microalgal biomass and thus primary production. Furthermore, benthic diatoms are able to quickly optimise their photosynthetic apparatus to the prevailing irradiance and thrive well under low-light conditions (Glud et al. 2002, Karsten et al. 2006, 2011). However, it is more likely that downward migration of the diatoms counteracts efficiently inhibiting light levels at the sediment surface (Kühl et al. 1996), so that benthic microalgal communities rarely exhibit photoinhibition or even photodamage (Serôdio et al. 1997, Consalvey 2002).

Based on our *in situ* NCP measurements, we constructed a mean regional *P/E* curve with the associated 95% confidence band. Using the *P/E* curve, in combination with several environmental parameters of the Arctic fjord, e.g. from monitoring data (solar radiation) and satellite data (SST), we were able to parameterise a numerical model to estimate the regional NCP rates of Kongsfjorden. The numerical model is a valuable tool to estimate regional rates of NCP and the impacts of temperature increases. The model estimated NCP rates for June 2008 between 15 and 18 mmol O_2 m^{-2} d^{-1} in the upper 10 to 15 m, which corresponds to mean hourly values of 0.6 to 0.8 mmol O_2 m^{-2} h^{-1}. These are in the same range as the maximally measured *in situ* values. We are aware that parameterisation of the *P/E* curve and temperature dependence are crucial for the modelling results. Therefore, we also performed sensitivity analyses of the model with respect to parameterisation of the *P/E* curve (i.e. the upper and lower 95% confidence curve) and temperature dependence of DCC and NCP (i.e. including uncertainties of the Q_{10} values). We were able to clearly demonstrate that uncertainties in Q_{10} values are highly relevant for the

model results. Thus, future studies examining highly variable parameters, such as temperature and light, need to be carried out in the field or laboratory. Consequently, the model still has a number of recognised limitations. Examples include the assumption of constant water transparency over the season (constant K_d values) and exclusion of temperature and light acclimation of the microalgae over the Arctic summer season. Because we could not parameterise these processes, they were not included in the model.

As vertical migration of microphytobenthos affects the determination of the light compensation point for microphytobenthic primary production, this value ranged from 15 to 24 µmol photons m^{-2} s^{-1} based on the regional *P/E* curves (Fig. 3). As incident PAR was minimal with 39 µmol photons m^{-2} s^{-1} at Arctic night times in June 2008, and because K_d was chosen to be 0.2 m^{-1}, modelled NCP was positive down to 20 to 25 m in June 2008 (Fig. 8). This compensation depth decreased to 15 m at the beginning and the end of the Arctic spring and summer seasons. NCP rates are negative in deeper waters where heterotrophic processes outbalance photoautotrophic processes (Fig. 8).

We investigated 2 hydrographical scenarios with the numerical model, which are assumed to represent the 2 extremes of natural mixing conditions in Kongsfjorden. Both scenarios define 2 very different temperature profiles. The water column in Kongsfjorden is stratified most of the summer season due to melting water from the glaciers (Hanelt et al. 2001). Our *in situ* temperature measurements in Kongsfjorden in June 2006, 2007 and 2008, on the other hand, showed relatively constant temperatures of 3.0 to 4.5°C at water depths below 5 m (Woelfel et al. 2009a, 2010, present study). However, as long as the frequency of certain hydrographical conditions (e.g. intrusion of Atlantic water) is not quantified for Kongsfjorden, the vertical temperature profile of this system is assumed to be somewhere between the stratified and fully mixed water column scenario. The satellite-derived SST values of the present study were averaged over the region (75.5 to 79.5° N and 8.0 to 12.0° E), i.e. a rather large area off Svalbard. Unfortunately, AMSR-E-satellite observations were not available for Kongsfjorden itself, partly due to the spatial resolution of the data (0.25°) and due to the close proximity to the sea ice and the coast. As the Westspitsbergen Current feeds into the outer fjord, the satellite data sufficiently reflect the SSTs of the outer fjord but overestimate the temperatures of the inner fjord. In the numerical model, the temperature of the stratified water column is higher than the mixed water column only in the upper 5 m. Temperature is always higher in the fully mixed scenario below this depth. Because we assumed constant temperature dependence (though different for DCC [Q_{10} = 2.4] and GCP [Q_{10} = 1.5]), the temperature differences of the 2 mixing scenarios directly determine modelled NCP rates. However, the modelled differences between the 2 mixing scenarios were small (in the range of 10%; Fig. 8E). Accordingly, depth-integrated NCP rates of the 2 mixing scenarios were similar and positive during the majority of the 2008 Arctic spring and summer seasons. The rates were negative (minimal -2×10^3 mol O_2 d^{-1}) only at the very beginning of April and during the last week of August 2008. The rates reached a maximum in June 2008 and ranged between 5×10^3 and 12×10^3 mol O_2 d^{-1}. The numerical model allowed us to simulate the effect of increasing SST by global warming. The estimated depth- and time-integrated, regional NCP rates were +9 and 30 t O_2 for June 2008 and the entire 2008 spring and summer seasons, respectively (Table 3). A suggested increase of summer SSTs by 2°C, according to the Intergovernmental Panel on Climate Change scenario (A1B in Christensen et al. 2007) and MacDonald (2010), would only have a marginal impact on the NCP rates of between −0.1 and +0.2% in June. The impact calculated for the entire spring and summer seasons would also be very small (−0.1%) for the stratified water column, as the temperature rise only affects the upper 3 to 5 m. In a mixed water column, where temperature linearly decreases with depth, a temperature increase would yield a slightly larger effect of −2.9%. The simulated decrease of NCP is mainly caused by the strong temperature dependence of DCC (Q_{10} = 2.4) and GCP (Q_{10} = 1.5).

It is likely that microphytobenthos production will rise as a consequence of the resulting increased light availability due to faster ice melting in spring and summer. On the other hand, the rising light availability will increase the competition for nutrients. Benthic microalgae exploit dissolved nutrients in pore and bottom water and thus successfully compete with the pelagic community (Glud et al. 2009). In contrast, pelagic phototrophs can better use the downwelling irradiance than communities constrained to a narrow zone on the sediment surface. Thus, nutrient availability regulates the relative importance of pelagic versus benthic microalgal productivity (Glud et al. 2009). Nevertheless, the extent to which benthic production matches planktonic production remains mostly unknown, especially in the Arctic (Krause-Jensen et al. 2007, Glud et al. 2009).

In conclusion, we found the new methodological approach of combining benthic chambers with optical oxygen sensors to be reliable in Arctic *in situ* conditions. The data clearly document a high abundance and production of benthic microalgae in Kongsfjorden and hence point to the important role of these organisms in trophic relationships under the harsh environmental conditions of the Arctic. The *in situ* measurements showed very high oxygen consumption rates of the entire benthic community, resulting in relatively low microphytobenthic NCP rates. The numerical model indicates only a minor impact of global warming on microphytobenthos production. However, there is an impact on the functioning and biogeochemistry of shallow pelagic ecosystems, but the question of whether their potential for carbon sequestration will be reduced (Schofield et al. 2010) or increased will be answered in the future.

Acknowledgements. This work was performed at the Ny-Ålesund International Arctic Environmental Research and Monitoring Facility under the agreement on scientific cooperation between the Alfred Wegener Institute and the University of Rostock. The authors thank the crew at the AWIPEV-base in Ny Ålesund and the German dive team (P. Leopold, M. Schwanitz, I. Vieweg) for assistance in the field, collecting the samples and further support in 2008. Special thanks to P. Leopold, J. Plößl, M. Schwanitz and M. Peterson for boat driving and measuring assistance. We are grateful to P. Kumm (workshop of the Institute of Chemistry, University of Rostock): all technical equipment for primary production *in situ* and *ex situ* measurements were manufactured by him. Thanks to M. Mann for determination of PON and POC, to S. Debatin (Alfred Wegener Institute Potsdam) for providing environmental data (global radiation, temperature, wind speed and direction) and to T. Seifert (Leibniz Institute for Baltic Sea Research) for processing Advanced Microwave Scanning Radiometer data. Financing and logistic support of our research in Ny Ålesund in 2008 was kindly provided by the European Center for Arctic Environmental Research (ARCFAC V; project no. 026129-02). Furthermore, we gratefully acknowledge financial support by the German Research Council (DFG, KA899/12-1/2/3). The authors thank 3 anonymous reviewers for helpful criticism on the manuscript.

LITERATURE CITED

Arrigo KR, van Dijken G, Pabi S (2008) Impact of a shrinking Arctic ice cover on marine primary production. Geophys Res Lett 35:L19603, doi:10.1029/2008GL035028

Brotas V, Plante-Cuny MR (1998) Spatial and temporal patterns of microphytobenthic taxa of estuarine tidal flats in the Tagus Estuary (Portugal) using pigment analysis by HPLC. Mar Ecol Prog Ser 171:43–45

Brotas V, Cabrita T, Portugal A, Serodio J, Catarino F (1995) Spatiotemporal distribution of the microphytobenthic biomass in intertidal flats of Tagus Estuary (Portugal). Hydrobiologia 301:93–104

Cahoon LB (1999) The role of benthic microalgae in neritic ecosystems. Oceanogr Mar Biol Annu Rev 37:47–86

Christensen JH, Hewitson B, Busuioc A, Chen A and others (2007) Regional climate projections. In: Solomon S, Qin D, Manning M, Chen Z and others (eds) Climate change 2007: the physical science basis. Contribution of Working Group I to the Fourth Assessment Report of the Intergovernmental Panel on Climate Change. Cambridge University Press, Cambridge, p 847–940

Consalvey M (2002) The structure and function of microphytobenthic biofilms. PhD thesis, University of St. Andrews

Forbes DL (2011) (ed) State of the Arctic coast 2010—scientific review and outlook. International Arctic Science Committee, Land-Ocean Interactions in the Coastal Zone, Arctic Monitoring and Assessment Programme, International Permafrost Association. Helmholtz Zentrum Geesthacht. LOICZ International Project Office, Geesthacht

Gilbert NS (1991) Primary production by benthic microalgae in nearshore marine sediments of Signy Island, Antarctica. Polar Biol 11:339–346

Glud RN, Kühl M, Wenzhöfer F, Rysgaard S (2002) Benthic diatoms of a high Arctic fjord (Young Sound, NE Greenland): importance for ecosystem primary production. Mar Ecol Prog Ser 238:15–29

Glud RN, Woelfel J, Karsten U, Kühl M, Rysgaard S (2009) Benthic microalgal production in the Arctic: applied methods and status of the current database. Bot Mar 52: 559–571

Hancke K, Glud RN (2004) Temperature effects on respiration and photosynthesis in three diatom-dominated benthic communities. Aquat Microb Ecol 37:265–281

Hanelt D, Tug H, Bischof K, Gross C, Lippert H, Sawall T, Wiencke C (2001) Light regime in an Arctic fiord: a study related to stratospheric ozone depletion as a basis for determination of UV effects on algal growth. Mar Biol 138:649–658

Hargrave BT, Prouse NJ, Phillips GA, Neame PA (1983) Primary production and respiration in the pelagic and benthic communities at 2 intertidal sites in the upper Bay of Fundy. Can J Fish Aquat Sci 40:s229–s243

Jeffrey SW, Humphrey GF (1975) New spectrophotometric equations for determining chlorophylls *a*, *b*, c_1 and c_2 in higher plants, algae and natural phytoplankton. Biochem Physiol Pflanz 167:191–194

Jesus B, Brotas V, Marani M, Paterson DM (2005) Spatial dynamics of microphytobenthos determined by PAM fluorescence. Estuar Coast Shelf Sci 60:30–42

Jørgensen BB, Nelson DC (2004) Sulfide oxidation in marine sediments: geochemistry meets microbiology. Geol Soc Am Bull 379:63–81

Karsten U, Schumann R, Rothe S, Jung I, Medlin L (2006) Temperature and light requirements for growth of two diatom species (Bacillariophyceae) isolated from an Arctic macroalga. Polar Biol 29:476–486

Karsten U, Schlie C, Woelfel J, Becker B (2011) Benthic diatoms in Arctic waters—ecological functions and adaptations. Polarforschung 81:77–84

Krause-Jensen D, Kühl M, Christensen PB, Borum J (2007) Benthic primary production in Young Sound, Northeast Greenland. In: Rysgaard S, Glud RN (eds) Carbon cycling in Arctic marine ecosystems: case study Young Sound. Meddelelser om Grønland. Bioscience Vol 58, p 160–173

Kühl M, Glud RN, Ploug H, Ramsing NB (1996) Microenvi-

ronmental control of photosynthesis and photosynthesis-coupled respiration in an epilithic cyanobacterial biofilm. J Phycol 32:799–812

Legendre P, Legendre L (2012) Numerical ecology, 3rd edn. Developments in environmental modelling, Vol 24. Elsevier, Amsterdam

Logan M (2010) Biostatistical design and analysis using R: a practical guide, 1st edn. Wiley-Blackwell, Oxford

MacDonald GM (2010) Global warming and the Arctic: a new world beyond the reach of the Grinnellian niche? J Exp Biol 213:855–861

MacIntyre HL, Geider RJ, Miller DC (1996) Microphytobenthos: the ecological role of the "secret garden" of unvegetated, shallow-water marine habitats. 1. Distribution, abundance and primary production. Estuaries 19:186–201

Morel A, Smith RC (1974) Relation between total quanta and total energy for aquatic photosynthesis. Limnol Oceanogr 19:591–600

Oksanen J, Guillaume Blanchet F, Kindt R, Legendre P and others (2012) Community ecology package. R package version 2.0-7. Available at http://CRAN.R-project.org/web/packages/vegan/index.html

Quinn GP, Keough KJ (2002) Experimental design and data analysis for biologists, 1st edn. Cambridge University Press, Cambridge

R Core Team (2013) R: a language and environment for statistical computing. R Foundation for Statistical Computing, Vienna. Available at www.R-project.org/

Rysgaard S, Nielsen TG, Hansen BW (1999) Seasonal variation in nutrients, pelagic primary production and grazing in a high-Arctic coastal marine ecosystem, Young Sound, Northeast Greenland. Mar Ecol Prog Ser 179:13–25

Sakshaug E (2004) Primary and secondary production in the Arctic seas. In: Stein R, MacDonald RW (eds) The organic carbon cycle in the Arctic Ocean. Springer, Berlin, p 57–81

Schippers A, Jørgensen BB (2001) Oxidation of pyrite and iron sulfide by manganese dioxide in marine sediments. Geochim Cosmochim Acta 65:915–922

Schofield O, Ducklow HW, Martinson DG, Meredith M, Moline MA, Fraser WR (2010) How do polar marine ecosystems respond to rapid climate change? Science 328: 1520–1523

Serôdio J, Marques Da Silva J, Catarino F (1997) Nondestructive tracing of migratory rhythms of intertidal benthic microalgae *in vivo* using chlorophyll *a* fluorescence. J Phycol 33:542–553

Spilmont N, Seuront L, Meziane T, Welsh DT (2011) There's more to the picture than meets the eye: sampling microphytobenthos in a heterogeneous environment. Estuar Coast Shelf Sci 95:470–476

Stroeve J, Holland MM, Meier W, Scambos T, Serreze M (2007) Arctic sea ice decline: faster than forecast. Geophys Res Lett 34:L09501, doi:10.1029/2007GL029703

Svendsen H, Beszczynska-Moller A, Hagen JO, Lefauconnier B and others (2002) The physical environment of Kongsfjorden-Krossfjorden, an Arctic fjord system in Svalbard. Polar Res 21:133–166

Tsubo M, Walker S (2005) Relationships between photosynthetically active radiation and clearness index at Bloemfontein, South Africa. Theor Appl Climatol 80:17–25

Underwood GJC, Kromkamp J (1999) Primary production by phytoplankton and microphytobenthos in estuaries. Adv Ecol Res 29:93–153

Verardo DJ, Froelich PN, Mcintyre A (1990) Determination of organic carbon and nitrogen in marine sediments using the Carlo Erba NA-1500 analyzer. Deep-Sea Res A 37:157–165

Walsby AE (1997) Numerical integration of phytoplankton photosynthesis through time and depth in a water column. New Phytol 136:189–209

Webb WL, Newton M, Starr D (1974) Carbon dioxide exchange of *Alnus rubra*: a mathematical model. Oecologia 17:281–291

Woelfel J, Schumann R, Leopold P, Wiencke C, Karsten U (2009a) Microphytobenthic biomass along gradients of physical conditions in Arctic Kongsfjorden, Svalbard. Bot Mar 52:573–583

Woelfel J, Sørensen K, Warkentin M, Forster S, Oren A, Schumann R (2009b) Oxygen evolution in a hypersaline crust: *in situ* photosynthesis quantification by microelectrode profiling and use of planar optode spots in incubation chambers. Aquat Microb Ecol 56:263–273

Woelfel J, Schumann R, Peine F, Flohr A and others (2010) Microphytobenthos of Arctic Kongsfjorden (Svalbard, Norway): biomass and potential primary production along the shore line. Polar Biol 33:1239–1253

Wulff A, Vilbaste S, Truu J (2005) Depth distribution of photosynthetic pigments and diatoms in the sediments of a microtidal fjord. Hydrobiologia 534:117–130

Editorial responsibility: Ronald Kiene, Mobile, Alabama, USA

Submitted: November 28, 2012; Accepted: December 9, 2013
Proofs received from author(s): March 6, 2014